

Quantitative Evaluation for Computational Cost of CG-FMM on Typical Wiregrid Models

Keisuke KONNO^{†a)}, Student Member, Qiang CHEN[†], Member, and Kunio SAWAYA[†], Fellow

SUMMARY The conjugate gradient-fast multipole method (CG-FMM) is one of the powerful methods for analysis of large-scale electromagnetic problems. It is also known that CPU time and computer memory can be reduced by CG-FMM but such computational cost of CG-FMM depends on shape and electrical properties of an analysis model. In this paper, relation between the number of multipoles and number of segments in each group is derived from dimension of segment arrangement in four typical wiregrid models. Based on the relation and numerical results for these typical models, the CPU time per iteration and computer memory are quantitatively discussed. In addition, the number of iteration steps, which is related to condition number of impedance matrix and analysis model, is also considered from a physical point of view.

key words: Method of Moments (MoM), conjugate gradient, fast multipole method

1. Introduction

The Method of Moments (MoM) is one of the powerful techniques for numerical analysis of antennas and scatterers [1], [2]. However, CPU time and computer memory to solve matrix equation in MoM by using conventional direct methods such as Gaussian elimination are proportional to $O(N^3)$ and $O(N^2)$, respectively, where N is the number of unknowns. Even though powerful computers with large memories are available, it is impossible to solve large-scale problems with millions of unknowns by the direct methods. Therefore, many techniques have been developed to reduce the CPU time and computer memory of MoM computation.

Iterative method such as the Conjugate Gradient (CG) method has been used to solve the MoM matrix equation in previous studies [3]–[8]. Unlike direct methods, the CPU time to solve the matrix equation by CG method is determined by number of iteration steps and CPU time per iteration. Therefore, computational cost of CG method is classified into three factors, i.e., the number of iteration steps, CPU time per iteration, and the computer memory. The number of iteration steps depends on the analysis model, while the CPU time per iteration and computer memory of CG method are both the order of $O(N^2)$.

In above three factors, the number of iteration steps of CG method has been discussed in a few papers so far and it has been reported that the number of iteration steps is strongly depended on the condition number of the

impedance matrix \mathbf{Z} [6]–[8]. But in these papers, little attention is paid to relation between the number of iteration steps and analysis model, as well as relation between condition number of \mathbf{Z} and analysis model.

On the other hand, it is known that other two factors except the number of iteration steps, namely, the CPU time per iteration and computer memory of CG method can be reduced by the Fast Multipole Method (FMM) [9], [10] or Multi-Level Fast Multipole Algorithm (MLFMA) [11]–[20]. It has been considered that the CPU time per iteration and computer memory of CG method combined with FMM (CG-FMM) are both $O(N^{1.5})$. However, the CPU time per iteration and computer memory in CG-FMM depend on many parameters for FMM as well as analysis model. Choice of parameters such as the number of multipoles or a group size for the two and three dimensional FMM have been discussed in a few papers [21], [22]. However, parameter choice based on these papers are not always correct in general since shape of analysis model, which is highly related to the number of multipoles L , has not been considered in these papers.

In this paper, four typical wiregrid models, which is formed electrically continuous or separated geometry, and one-dimensional or two-dimensional geometry, are introduced. It is shown that relation between the number of multipoles L and number of segments in each group K is determined by dimension of segment arrangement in an analysis model, and the relation is used to discuss not only the CPU time per iteration but also the computer memory required for analysis. Based on numerical simulation for these typical models, mutual relation among the number of iteration steps, condition number of \mathbf{Z} and analysis model can be discussed universally from a physical point of view.

This paper is organized as follows. Section 2 presents principle of CG-FMM and important parameters related to the computational cost. In Sect. 3, four typical models and two different relations between L and K are shown. In Sect. 4, the computational cost of CG-FMM for these typical models is discussed theoretically and numerically.

2. Principle of CG-FMM

2.1 Conjugate Gradient Method

Matrix equation produced by the MoM is expressed by

$$\mathbf{Z}\mathbf{I} = \mathbf{V}, \quad (1)$$

where \mathbf{Z} is $N \times N$ impedance matrix produced by the MoM,

Manuscript received January 4, 2010.

Manuscript revised May 4, 2010.

[†]The authors are with the Department of Electrical Communications Engineering, Graduate School of Engineering, Tohoku University, Sendai-shi, 980-8579 Japan.

a) E-mail: konno@ecei.tohoku.ac.jp

DOI: 10.1587/transcom.E93.B.2611

\mathbf{V} is N -dimensional known voltage vector, and \mathbf{I} is N -dimensional unknown current vector. The algorithm of CG method for solving Eq. (1) is summarized as follows [3]–[8].

CG method for MoM.

- After initial value of \mathbf{I} is set to be \mathbf{I}_0 , initial value of residual vector \mathbf{R}_0 and correction vector for solution \mathbf{P}_0 are calculated as

$$\mathbf{R}_0 = \mathbf{V} - \mathbf{Z}\mathbf{I}_0,$$

$$\mathbf{P}_0 = \mathbf{Z}^\dagger \mathbf{R}_0.$$

- Iterations ($i = 1, 2, \dots$) are stopped after the desired residual norm $\|\mathbf{R}_i\|$ is obtained as

$$\alpha_i = \frac{\langle \mathbf{Z}\mathbf{P}_{i-1}, \mathbf{R}_{i-1} \rangle}{\|\mathbf{Z}\mathbf{P}_{i-1}\|^2} = \frac{\|\mathbf{Z}^\dagger \mathbf{R}_{i-1}\|^2}{\|\mathbf{Z}\mathbf{P}_{i-1}\|^2},$$

$$\mathbf{I}_i = \mathbf{I}_{i-1} + \alpha_i \mathbf{P}_{i-1},$$

$$\mathbf{R}_i = \mathbf{V} - \mathbf{Z}\mathbf{I}_i = \mathbf{R}_{i-1} - \alpha_i \mathbf{Z}\mathbf{P}_{i-1}.$$

If $\|\mathbf{R}_i\| < \epsilon \|\mathbf{V}\|$, iteration is stopped.

$$\beta_i = \frac{\|\mathbf{Z}^\dagger \mathbf{R}_i\|^2}{\|\mathbf{Z}^\dagger \mathbf{R}_{i-1}\|^2},$$

$$\mathbf{P}_i = \mathbf{Z}^\dagger \mathbf{R}_i + \beta_i \mathbf{P}_{i-1},$$

where α_i and β_i are correction coefficients for \mathbf{I}_{i-1} and \mathbf{P}_{i-1} , respectively, and ϵ is an error control parameter for the solution. \mathbf{Z}^\dagger denotes the conjugate transpose of \mathbf{Z} .

In the above algorithm, two times of matrix-vector multiplication are carried out in each iteration and CPU time for the matrix-vector multiplication is $O(N^2)$. In addition, computer memory for storing \mathbf{Z} is also $O(N^2)$.

2.2 Fast Multipole Method

FMM is a method based on the addition theorem of the scalar Green's function [9], [10]. FMM can reduce both the CPU time for the matrix-vector multiplication and computer memory of CG method to $O(N^{1.5})$ when number of groups $M = \sqrt{N}$. The matrix-vector multiplication in each step of CG-FMM can be collectively carried out by grouping scheme based on the addition theorem. In addition, mutual impedance between far segments are calculated by the addition theorem at every time of the matrix-vector multiplication in CG-FMM and the full impedance matrix \mathbf{Z} is not necessary to be stored. In what follows, formulation of the mutual impedance between far segments based on FMM is explained.

In the Galerkin-MoM, the expression of the mutual impedance between far segments is obtained as

$$Z_{mkm'k'}^{\text{far}} = j\omega\mu_0 \int_{l_{mk}} \mathbf{f}_{mk}(\mathbf{r}_k) \cdot \int_{l_{m'k'}} \overline{\mathbf{G}}_0(\mathbf{r}_k, \mathbf{r}_{k'}) \cdot \mathbf{f}_{m'k'}(\mathbf{r}_{k'}) d\mathbf{r}' d\mathbf{r}, \quad (2)$$

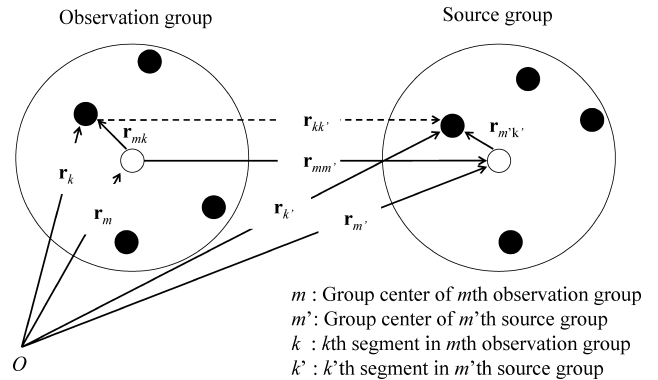


Fig. 1 Definition of vectors and subscripts for FMM formulation.

where m and $m' (= 1, 2, \dots, M)$ are observation group number and source group number, respectively [1]. k and $k' (= 1, 2, \dots, N/M (= K))$ represent segment number in m th observation group and m' th source group, respectively. Here, M is the total number of groups and K is the total number of segments in each group. l_{mk} and $l_{m'k'}$ denote the path of integration along the observation segment and source segment. Figure 1 shows the definition of vectors and subscripts.

When $|\mathbf{r}_{mm'}| \gg |\mathbf{r}_{m'k'} - \mathbf{r}_{mk}|$, the Gegenbauer's addition theorem [23] and plane wave expansion for spherical waves can be applied to Eq. (2) and

$$Z_{mkm'k'}^{\text{far}} \approx \frac{\omega\mu_0 k_0}{(4\pi)^2} \int_0^{2\pi} \int_0^\pi \mathbf{s}_{mk}(\hat{\mathbf{k}}) T_{mm'} \mathbf{s}_{m'k'}^*(\hat{\mathbf{k}}) \sin\theta d\theta d\phi, \quad (3)$$

is obtained, where $\mathbf{s}_{mk}(\hat{\mathbf{k}})$, $\mathbf{s}_{m'k'}(\hat{\mathbf{k}})$, and $T_{mm'}$ are expressed as follows.

$$\mathbf{s}_{mk}(\hat{\mathbf{k}}) = \int_{l_{mk}} e^{j\mathbf{k} \cdot \mathbf{r}_{mk}} (\overline{\mathbf{I}} - \hat{\mathbf{k}}\hat{\mathbf{k}}) \cdot \mathbf{f}_{mk}(\mathbf{r}_k) d\mathbf{r}_k. \quad (4)$$

$$\mathbf{s}_{m'k'}(\hat{\mathbf{k}}) = \int_{l_{m'k'}} e^{j\mathbf{k} \cdot \mathbf{r}_{m'k'}} (\overline{\mathbf{I}} - \hat{\mathbf{k}}\hat{\mathbf{k}}) \cdot \mathbf{f}_{m'k'}(\mathbf{r}_{k'}) d\mathbf{r}_{k'}. \quad (5)$$

$$T_{mm'} = \sum_{l=0}^L (-j)^l (2l+1) h_l^{(2)}(k_0 r_{mm'}) P_l(\hat{\mathbf{k}} \cdot \hat{\mathbf{r}}_{mm'}). \quad (6)$$

$\mathbf{s}_{mk}(\hat{\mathbf{k}})$, called “receiving function” means the mutual impedance between the center of the m th observation group and k th segment in m th group. $\mathbf{s}_{m'k'}(\hat{\mathbf{k}})$, called “radiation function” means the mutual impedance between the center of the m' th source group and k' th segment in m' th group. $T_{mm'}$, called “transfer function” represents the mutual impedance between the center of the m th observation group and that of the m' th source group. $\overline{\mathbf{I}} = \hat{\mathbf{x}}\hat{\mathbf{x}} + \hat{\mathbf{y}}\hat{\mathbf{y}} + \hat{\mathbf{z}}\hat{\mathbf{z}}$ denotes the unit dyad and $\hat{\mathbf{k}} = \hat{\mathbf{x}} \sin\theta \cos\phi + \hat{\mathbf{y}} \sin\theta \sin\phi + \hat{\mathbf{z}} \cos\theta$ is a unit vector of radial direction on a unit sphere. $h_l^{(2)}$ is the l th order spherical Hankel function of the second kind and P_l is the Legendre polynomial of l th order.

Equation (6) is a finite series whose summation is truncated at L . The truncation number L is given by a following empirical formula

$$L = k_0 D_{\text{max}} + \alpha_L \ln(k_0 D_{\text{max}} + \pi), \quad (7)$$

Table 1 CPU time for matrix-vector multiplication in CG-FMM.

Type of multiplication	Step	CPU time
Multiplication for Z^{near}		$O(MK^2)$
Multiplication for Z^{far}	Step 1	$O(2NL^2)$
	Step 2	$O(2M^2L^2)^*$
	Step 3	$O(2NL^2)$

* CPU time for Step 2 is dominant in the most cases of large-scale models.

where D_{max} is the maximum diameter of the groups and $\alpha_L (= 0 \sim 10)$ is the error control parameter for the transfer function. In addition, L is also used for the points of double numerical integration in Eq. (3). In order to obtain accurate results, L point Gauss-Legendre integration in θ and $2L$ point trapezoidal integration in ϕ are applied to Eq. (3). Namely, each component of $\mathbf{s}_{mk}(\hat{\mathbf{k}})$, $\mathbf{s}_{m'k'}(\hat{\mathbf{k}})$ as well as $T_{mm'}$ are stored as $L \times 2L = 2L^2$ discrete data in numerical calculation.

According to above formulae, the matrix-vector multiplication for the mutual impedance elements between far segments in CG-FMM is represented by following three steps.

Step 1 Aggregation step ($m' = 1, \dots, M$)

$$\mathbf{S}_{m'}(\hat{\mathbf{k}}) = \sum_{k'=1}^K \mathbf{s}_{m'k'}(\hat{\mathbf{k}}) a_{k'}. \quad (8)$$

In m' th source group, the radiation function $\mathbf{s}_{m'k'}(\hat{\mathbf{k}})$ is multiplied by $a_{k'}$, which is k' th component of a vector \mathbf{a} , and results of the multiplication are stored. Here, \mathbf{a} is \mathbf{I} , \mathbf{R} , or \mathbf{P} (see Sect. 2.1) in CG-FMM. Since the aggregation step is applied to all N radiation function, the CPU time for the aggregation step is $O(N \times 2L^2)$.

Step 2 Translation step ($m = 1, \dots, M$)

$$\mathbf{S}_m(\hat{\mathbf{k}}) = \sum_{\substack{m'=1 \\ m' \in M_{\text{far}}}}^M \mathbf{S}_{m'}(\hat{\mathbf{k}}) T_{mm'}(k_0 r_{mm'}, \hat{\mathbf{k}} \cdot \hat{\mathbf{r}}_{mm'}). \quad (9)$$

$\mathbf{S}_{m'}(\hat{\mathbf{k}})$ is transferred to the center of m th observation group by the transfer function $T_{mm'}$. M_{far} denotes all far groups from m th observation group. This translation step from M source groups is repeated for all M observation groups and the total CPU time for the translation step is $O(M^2 \times 2L^2)$.

Step 3 Disaggregation step ($i = 1, \dots, N$)

$$\sum_{\substack{j=1 \\ j \in N_{\text{far}}}}^N Z_{ij}^{\text{far}} a_j \approx \frac{\omega \mu_0 k_0}{(4\pi)^2} \sum_{\theta=1}^L \sum_{\phi=1}^{2L} W(\theta) \frac{\pi}{L} [\mathbf{s}_{mk}(\hat{\mathbf{k}}) \cdot \mathbf{S}_m(\hat{\mathbf{k}})]. \quad (10)$$

The multiplication for Z^{far} in the i th row of the impedance matrix is collectively calculated by right-hand side. Here,

Table 2 Computer memory for CG-FMM.

Stored contents	Computer memory
$\mathbf{V}, \mathbf{I}, \mathbf{P}, \mathbf{R}$	$O(N)$
$W(\theta)$	$O(L)$
$Z_{mkm'k'}^{\text{near}}$	$O(MK^2)$
$\mathbf{s}_{mk}(\hat{\mathbf{k}})$ and $\mathbf{s}_{m'k'}(\hat{\mathbf{k}})$	$O(2NL^2)$
$T_{mm'}(k_0 r_{mm'}, \hat{\mathbf{k}} \cdot \hat{\mathbf{r}}_{mm'})$	$O(2M^2L^2)$

N_{far} denotes all far segments from segments in the m th observation group, and $W(\theta)$ is the weight of Gauss-Legendre integration in θ . The disaggregation step is carried out for all N rows of the impedance matrix and the CPU time for the disaggregation step is $O(N \times 2L^2)$.

The CPU time for all steps in the multiplication of Z^{near} , which denotes the mutual impedance between near segments, and that of Z^{far} are shown in Table 1. The computer memory for CG-FMM is also tabulated in Table 2.

3. Typical Models

Four typical models described in the paper are shown in Fig. 2. Figure 2(a) shows one-dimensional side-by-side dipole array antenna (Model 1), where dipole element, whose length is l and radius is a , is arrayed periodically. Each element is divided into K wire segments. Periodicity of the group and segment location are both satisfied in this model.

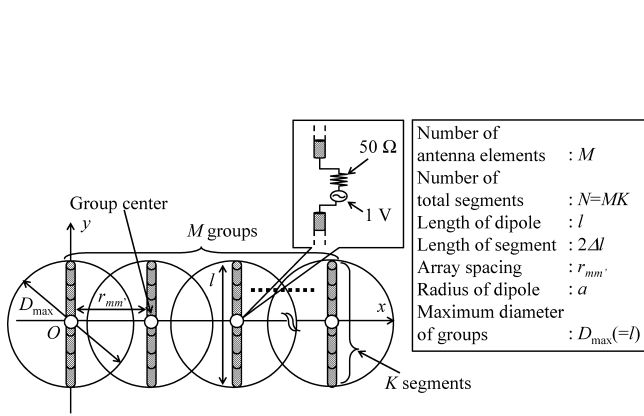
Figure 2(b) shows long dipole antenna (Model 2), whose length is $l (\gg \lambda)$ and radius is a . The dipole antenna is divided into N wire segments. Periodicity of the group and segment location are both satisfied in this model.

Figure 2(c) shows two-dimensional planar array of conducting scatterers (Model 3). A planar element, whose size is $d_x \times d_y$, is arrayed periodically. Each element is divided into K wire segments with radius a . Periodicity of the group and segment location are both satisfied in this model.

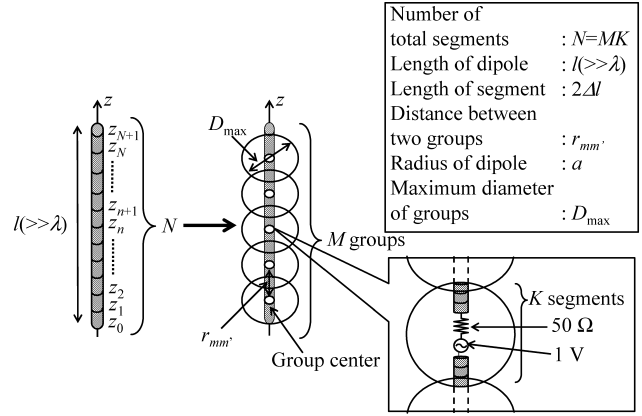
Figure 2(d) shows planar conductor (Model 4). A planar element, whose size is $d_x \times d_y$, is divided into N wire segments with radius a . Periodicity of the group location is only satisfied in this model. Since the uniform grouping for segments is difficult, non-uniform grouping scheme and versatile program using CG-FMM is used for analysis of the model.

Relation between the number of multipoles L and segments in each group K is shown in Table 3. In general, K is proportional to D_{max}^2 for two-dimensional arrangement, while K is proportional to D_{max} for one-dimensional arrangement. Substituting the relation between K and D_{max} into Eq. (7), the relation between L and K shown in Table 3 can be easily derived.

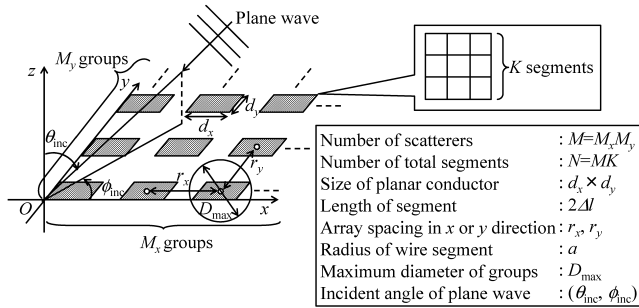
As shown in Table 4, the use of periodicity in CG-FMM can reduce the computer memory required for analysis. By using Tables 2–4, the computer memory required for CG-FMM corresponding to each analysis model can be easily obtained. In a similar way, CPU time per iteration in CG-FMM can be also obtained from Tables 1 and 3.



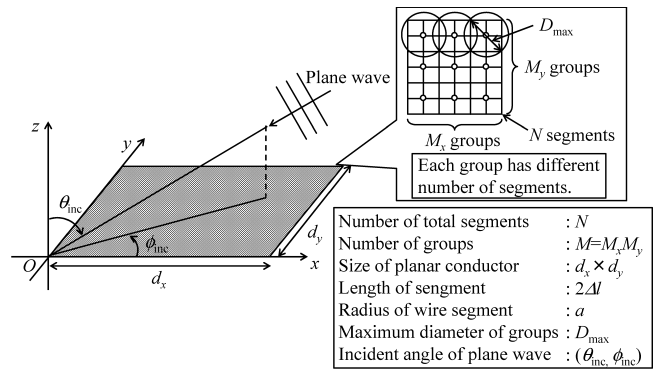
(a) One-dimensional side-by-side dipole array antenna (Model 1).



(b) Long dipole antenna (Model 2).



(c) Two-dimensional array of planar scatterers (Model 3).



(d) Planar scatterer (Model 4).

Fig. 2 Four typical wiregrid models.

Table 3 Relation between L and K .

Segment arrangement	Relation between L and K
1D (Models 1 and 2)	$L \propto K$
2D (Models 3 and 4)	$L^2 \propto K$

Table 4 Computer memory reduction using periodicity in CG-FMM.

Type of periodicity in analysis model	Required computer memory		
	$Z_{mkm'k'}^{near}$	$T_{mm'}$	$S_{mk}, S_{m'k'}$
None	$O(MK^2)$	$O(2M^2L^2)$	$O(2NL^2)$
Group location	$O(MK^2)$	$O(2ML^2)$	$O(2NL^2)$
Group and segment location	$O(K^2)$	$O(2ML^2)$	$O(2KL^2)$

4. Numerical Results

In this section, numerical analysis of four typical models is carried out using the Richmond's MoM [2]. Dell Precision PWS 380 with 2 GB RAM is used for all numerical calcu-

lation. $\epsilon = 10^{-4}$ is used for the convergence criterion of CG-FMM and $\alpha_L = 2$ is employed to Eq. (7) for sufficient truncation number. In addition, the self impedance and the mutual impedance between segments in adjacent groups are calculated by the MoM, rather than by FMM. Initial value of current vector \mathbf{I} is zero vector. Preconditioning technique is not used in both CG method and CG-FMM.

4.1 Number of Iteration Steps and Condition Number

The number of iteration steps required for CG method and CG-FMM and the condition number κ of \mathbf{Z} for four typical models are shown in Fig. 3. The condition number κ of \mathbf{Z} is defined by

$$\kappa = \sqrt{\frac{\lambda_{\max}}{\lambda_{\min}}} \quad (11)$$

where λ_{\max} and λ_{\min} are the maximum and minimum eigenvalue of $\mathbf{Z}^\dagger \mathbf{Z}$, respectively. As shown in Fig. 3, the tendency of the condition number κ is almost the same to that of the number of iteration steps determined by error control parameter. From those results, it is found that the condition

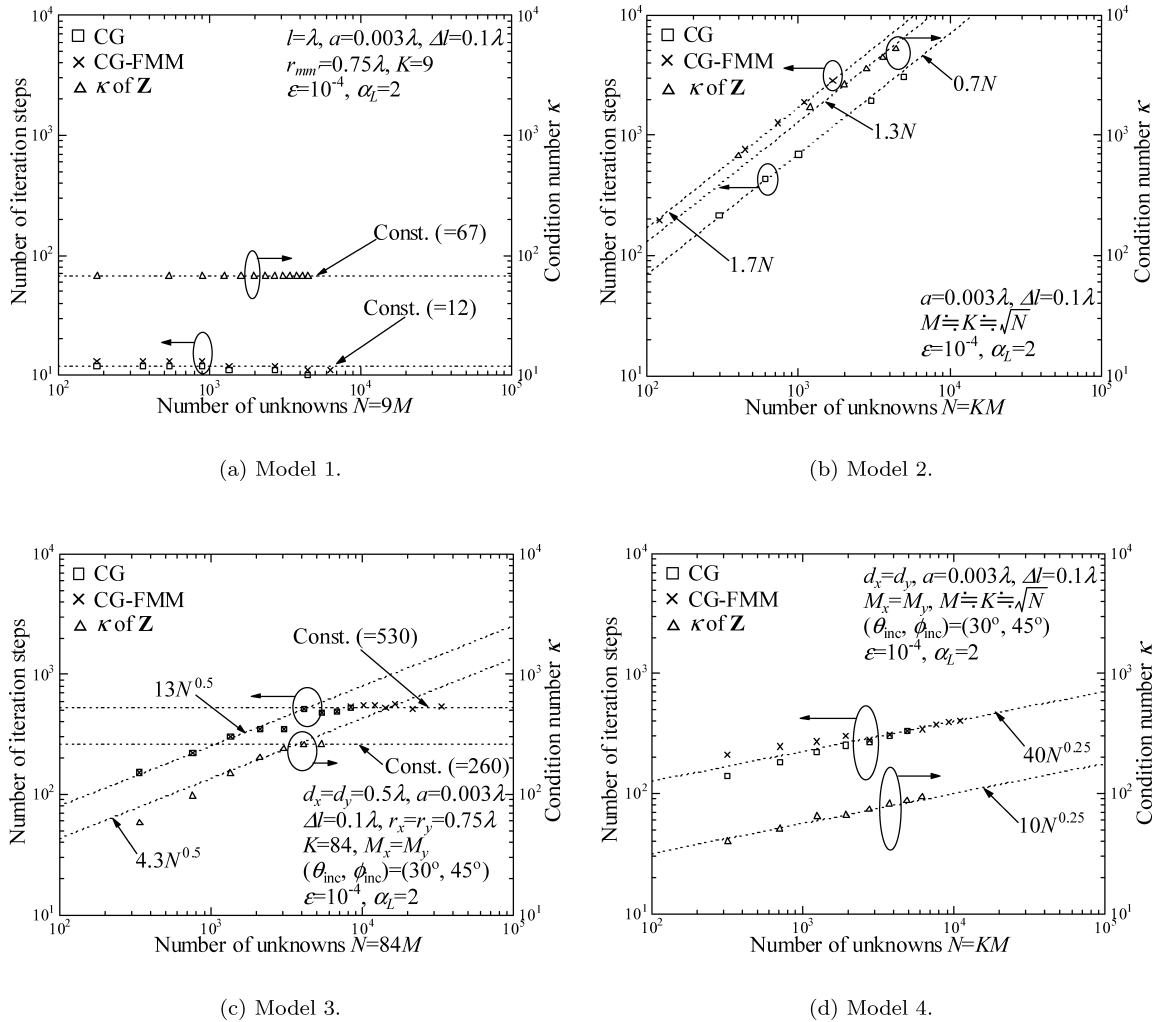


Fig. 3 Number of iteration steps and condition number of \mathbf{Z} .

number is highly related to that of the number of iteration steps.

Large κ means that the impedance matrix \mathbf{Z} is ill-conditioned and convergence of the solution obtained in iterative procedure is slow. On the other hand, small κ means that the impedance matrix \mathbf{Z} is well-conditioned and convergence of the solution is fast.

From a physical point of view, condition number κ indicates how the solution \mathbf{I} in Eq. (1) is sensitive to the values of the elements in the impedance matrix \mathbf{Z} . When electrical connection between segments in the model is strong due to linear-connection of segments or strong mutual coupling such as Models 2 and 3, the condition number κ increases as shown in Figs. 3(b) and 3(c), and \mathbf{I} is sensitive to \mathbf{Z} . On the other hand, when electrical connection between segments in the model is weak due to small mutual coupling or grid-connection of segments such as Models 1 and 4, condition number κ is small as shown in Figs. 3(a) and 3(d), and \mathbf{I} is not sensitive to \mathbf{Z} . Constant κ shown in Figs. 3(a) and 3(c) means that mutual coupling effect to an element does not change anymore even if M increases. In general, since current of each segment is affected by all segments, the num-

ber of iteration steps required for analysis increases when number of segments N increases. However, mutual coupling effect to \mathbf{I} from significantly far elements is very small and negligible in the array antenna such as Models 1 and 3. Therefore, κ and number of iteration steps required for analysis of the array antenna which has enough number of elements becomes constant.

4.2 CPU Time per Iteration

The CPU time per iteration for analysis of four typical models is shown in Fig. 4. It is found that the CPU time per iteration of CG-FMM is $O(N^2)$ for the Models 1 and 2, while that for the Models 3 and 4 is reduced to $O(N^{1.5})$. Using $L \propto K$ shown in Table 3, it can be derived from Table 1 that the CPU time per iteration for analysis of one-dimensional models is $O(N^2)$, which is independent of the value of M , because the CPU time of Step 2 in Table 1 is $O(N^2)$. In Fig. 4(c), the order of the CPU time per iteration is $O(N)$, when N is small. Since K is constant ($= 84$) in the model 3, it is easy to understand that $K \gg M$ when $N(= MK)$ is as small as about 1000 or less. Based on $L^2 \propto K$ shown in

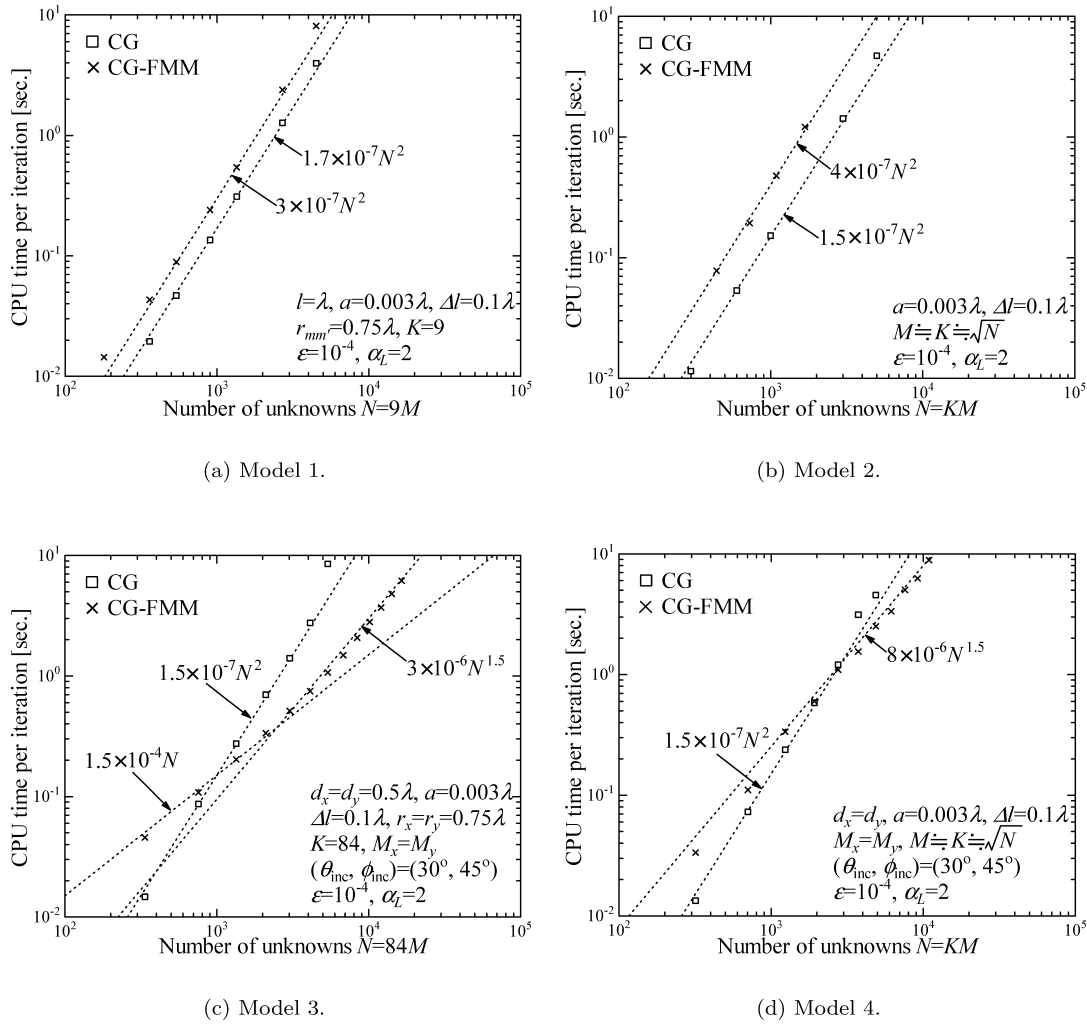


Fig. 4 CPU time per iteration for analysis.

Table 5 Computational cost of CG-FMM for four typical wiregrid models.

Item		Model 1	Model 2	Model 3	Model 4
Properties of analysis model	Segment arrangement	1D	1D	2D	2D
	Segment connection	Linearly connected	Linearly connected	Grid connected	Grid connected
	Number of elements	Array	Single	Array	Single
Type of periodicity used in CG-FMM	Group location	Used	Used	Used	Used
	Segment location	Used	Used	Used	Not used
Relation between L and K		$L \propto K$	$L \propto K$	$L^2 \propto K$	$L^2 \propto K$
Parameter setting on grouping		$K = \text{Const.}$	$M = K = \sqrt{N}$	$K = \text{Const.}$	$M = K = \sqrt{N}$
Computational cost	Number of iteration steps	Const.	$O(N)$	$O(N^{0.5}) \rightarrow \text{Const.}$	$O(N^{0.25})$
	CPU time per iteration	$O(N^2)$	$O(N^2)$	$O(N) \rightarrow O(N^{1.5})$	$O(N^{1.5})$
	Total CPU time	$O(N^2)$	$O(N^3)$	$O(N^{1.5})$	$O(N^{1.75})$
	Computer memory	$O(K^3) \rightarrow O(N)$	$O(N^{1.5})$	$O(K^2) \rightarrow O(N)$	$O(N^{1.5})$

Table 3 and $K(= \text{Const.}) \gg M$, it can be obtained from Table 1 that the CPU time per iteration for analysis of model 3 is $O(N)$ when N is small. From these results, it is concluded that the CPU time per iteration to analyze an antenna which has one-dimensional segment arrangement can not be reduced by CG-FMM.

4.3 Computer Memory

The order of the computer memory required for analysis of each model can be theoretically derived from Tables 2–4 without running programs and is tabulated in Table 5. From

the Table 5, it is found that the computer memory required for analysis of any models is smaller than $O(N^2)$ in CG-FMM. For the array antenna/scatterer such as the Models 1 and 3, the computer memory for s_{mk} and $s_{m'k'}$ is dominant for the total computer memory when M is very small. On the other hand, the computer memory for T_{mn} is dominant for the total computer memory when M is larger than K . Therefore, the order of the computer memory required for analysis varies as $O(K^3) \rightarrow O(N)$ for Model 1 and $O(K^2) \rightarrow O(N)$ for Model 3.

The order of the number of iteration steps, CPU time per iteration, total CPU time and computer memory is tabulated in Table 5.

5. Conclusion

In this paper, relation between the computational cost of CG-FMM and the analysis model was quantitatively evaluated by numerical simulation for four typical wire antennas or wiregrid models. It is found that the number of iteration steps required for analysis by CG-FMM depends on the condition number of \mathbf{Z} . From discussion of relation between the condition number κ and electrical properties of the models, it is shown that the condition number κ becomes large due to linear-connection of segments or strong mutual coupling between elements. Similarly, it is shown that the condition number κ becomes small due to grid-connection of segments exist or weak mutual coupling between elements. The computer memory required for analysis are reduced from $O(N^2)$ for all models by the use of CG-FMM. On the other hand, it is shown that the CPU time per iteration can be reduced only for models which has two-dimensional segment arrangement in each group.

Since the models for analysis used in this paper are simple linear or planar models, the computational cost of CG-FMM for more complicated structures is desired to be evaluated. In addition, the computational cost of CG-FMM applied to the Rao-Wilton-Glisson (RWG) basis function [24] as well as the Schaubert-Wilton-Glisson (SWG) basis function [25] is expected to be evaluated for analysis of structures including dielectric bodies.

Acknowledgments

This work was supported by the GCOE Program CERIES in Tohoku University, and SCAT (Support Center for Advanced Telecommunications) Technology Research, Foundation. Supercomputing resources at Cyberscience Center in Tohoku University were used in process of this research.

References

- [1] R.F. Harrington, *Field Computation by Moment Methods*, Macmillan, New York, 1968.
- [2] J.H. Richmond and N.H. Greay, "Mutual impedance of nonplanar-skew sinusoidal dipoles," *IEEE Trans. Antennas Propag.*, vol.AP-23, no.5, pp.412–414, May 1975.
- [3] T.K. Sarkar and S.M. Rao, "The application of the conjugate gradient method for the solution of electromagnetic scattering from arbitrarily oriented wire antennas," *IEEE Trans. Antennas Propag.*, vol.AP-32, no.4, pp.398–403, April 1984.
- [4] T.K. Sarkar, "The conjugate gradient method as applied to electromagnetic field problems," *IEEE Antennas Propagation Society Newsletter*, vol.28, no.4, pp.4–14, Aug. 1986.
- [5] J. Tang, "Numerical aspects of iterative solving of linear systems derived from Helmholtz's problem," Literature Report of Delft University of Technology, Feb. 2004.
- [6] T.K. Sarkar, K.R. Siarkiewicz, and S.M. Rao, "Survey of numerical methods for solution of large systems of linear equations for electromagnetic field problems," *IEEE Trans. Antennas Propag.*, vol.AP-29, no.6, pp.847–856, Nov. 1981.
- [7] A.F. Peterson and R. Mittra, "Convergence of the conjugate gradient method when applied to matrix equations representing electromagnetic scattering problems," *IEEE Trans. Antennas Propag.*, vol.AP-34, no.12, pp.1447–1454, Dec. 1986.
- [8] A.F. Peterson, C.F. Smith, and R. Mittra, "Eigenvalues of the moment-method matrix and their effect on the convergence of the conjugate gradient algorithm," *IEEE Trans. Antennas Propag.*, vol.36, no.8, pp.1177–1179, Aug. 1988.
- [9] R. Coifuman, V. Rokhlin, and S. Wandzura, "The fast multipole method for the wave equation: A pedestrian prescription," *IEEE Antennas Propag. Mag.*, vol.35, no.3, pp.7–12, June 1993.
- [10] V. Rokhlin, "Rapid solution of integral equations of scattering theory in two dimension," *J. Comput. Phys.*, vol.86, no.2, pp.414–439, Feb. 1990.
- [11] J.M. Song and W.C. Chew, "Multilevel fast-multipole algorithm for solving combined field integral equations of electromagnetic scattering," *Microw. Opt. Technol. Lett.*, vol.10, no.1, pp.14–19, Sept. 1995.
- [12] J.M. Song, C.C. Lu, and W.C. Chew, "Multilevel fast multipole algorithm for electromagnetic scattering by large complex objects," *IEEE Trans. Antennas Propag.*, vol.45, no.10, pp.1488–1493, Oct. 1997.
- [13] I. Bogaert, J. Peeters, and F. Olyslager, "A nondirective plane wave MLFMA stable at low frequencies," *IEEE Trans. Antennas Propag.*, vol.56, no.12, pp.3752–3767, Dec. 2008.
- [14] J. Fostier and F. Olyslager, "An asynchronous parallel MLFMA for scattering at multiple dielectric objects," *IEEE Trans. Antennas Propag.*, vol.56, no.8, pp.2346–2355, Aug. 2008.
- [15] O. Ergul and L. Gurel, "Efficient parallelization of the multilevel fast multipole algorithm for the solution of large-scale scattering problems," *IEEE Trans. Antennas Propag.*, vol.56, no.8, pp.2335–2345, Aug. 2008.
- [16] O. Ergul and L. Gurel, "Comparison of integral-equation formulations for the fast and accurate solution of scattering problems involving dielectric objects with the multilevel fast multipole algorithm," *IEEE Trans. Antennas Propag.*, vol.57, no.1, pp.176–187, Jan. 2009.
- [17] A. Tzoulis and T.F. Eibert, "Efficient electromagnetic near-field computation by the multilevel fast multipole method employing mixed near-field/far-field translations," *IEEE Antennas Wireless Propag. Lett.*, vol.4, pp.449–452, 2005.
- [18] Ismatullah and T.F. Eibert, "Surface integral equation solutions by hierarchical vector basis functions and spherical harmonics based multilevel fast multipole method," *IEEE Trans. Antennas Propag.*, vol.1, no.1, pp.1–14, Jan. 2010.
- [19] I. Hanninen and J. Sarvas, "Efficient evaluation of the Rokhlin translator in multilevel fast multipole algorithm," *IEEE Trans. Antennas Propag.*, vol.56, no.8, pp.2356–2362, Aug. 2008.
- [20] T. Dufva and J. Sarvas, "Broadband MLFMA with plane wave expansions and optimal memory demand," *IEEE Trans. Antennas Propag.*, vol.57, no.3, pp.742–753, March 2009.
- [21] S.S. Bindiganavale and J.L. Volakis, "Guidelines for using the fast multipole method to calculate the RCS of large objects," *Microw. Opt. Technol. Lett.*, vol.11, no.4, pp.190–194, March 1996.

- [22] Z. Yaojiang, G. Zhonglin, Z. Lezhu, and F. Zhenghe, "Guidelines of parameter settings in 3D fast multipole method," Proc. ICMMT2000, pp.387-390, Beijing, China, Sept. 2000.
- [23] M. Abramowitz and I.A. Stegun, Handbook of Mathematical Functions, National Bureau of Standards, 1972.
- [24] S.M. Rao, D.R. Wilton, and A.W. Glisson, "Electromagnetic scattering by surfaces of arbitrary shape," IEEE Trans. Antennas Propag., vol.AP-30, no.3, pp.409-418, May 1982.
- [25] D.H. Schaubert, D.R. Wilton, and A.W. Glisson, "A tetrahedral modeling method for electromagnetic scattering by arbitrarily shaped inhomogeneous dielectric bodies," IEEE Trans. Antennas Propag., vol.AP-32, no.1, pp.77-85, Jan. 1984.



Keisuke Konno received the B.E. and M.E. degrees from Tohoku University, Sendai, Japan, in 2007 and 2009, respectively. Currently, he works for the D.E. degree at the Department of Electrical Communication Engineering in Graduate School of Engineering, Tohoku University. His research interests include computational electromagnetics, array antennas.



Qiang Chen received the B.E. degree from Xidian University, Xi'an, China, in 1986, the M.E. and D.E. degrees from Tohoku University, Sendai, Japan, in 1991 and 1994, respectively. He is currently an Associate Professor with the Department of Electrical Communications, Tohoku University. His primary research interests include computational electromagnetics, array antennas, and antenna measurement. Dr. Chen received the Young Scientists Award in 1993, the Best Paper Award in 2008 from the Institute of Electronics, Information and Communication Engineers (IEICE) of Japan.

Dr. Chen is a member of the IEEE. He has served as the Secretary and Treasurer of IEEE Antennas and Propagation Society Japan Chapter in 1998, the Secretary of Technical Committee on Electromagnetic Compatibility of IEICE from 2004 to 2006. He is now the Secretary of Technical Committee on Antennas and Propagation of IEICE, Associate Editor of IEICE Transactions on Communications.



Kunio Sawaya received the B.E., M.E. and D.E. degrees from Tohoku University, Sendai, Japan, in 1971, 1973 and 1976, respectively. He is presently a Professor in the Department of Electrical and Communication Engineering at the Tohoku University. His areas of interests are antennas in plasma, antennas for mobile communications, theory of scattering and diffraction, antennas for plasma heating, and array antennas. He received the Young Scientists Award in 1981, the Paper Award in 1988, Communications Society Excellent Paper Award in 2006, and Zen-ichi Kiyasu Award in 2009 all from the Institute of Electronics, Information and Communication Engineers (IEICE). He served as the Chairperson of the Technical Group of Antennas and Propagation of IEICE from 2001 to 2003, the Chairperson of the Organizing and Steering Committees of 2004 International Symposium on Antennas and Propagation (ISAP'04) and the President of the Communications Society of IEICE from 2009 to 2010. Dr. Sawaya is a senior member of the IEEE, and a member of the Institute of Image Information and Television Engineers of Japan.

Dr. Sawaya is a senior member of the IEEE, and a member of the Institute of Image Information and Television Engineers of Japan.